J. Synchrotron Rad. (1998). **5**, 1–5

Two-Plane Focusing of 30 keV Undulator Radiation

P. Elleaume

European Synchrotron Radiation Facility, BP 220, F-38043 Grenoble CEDEX, France. E-mail: elleaume@esrf.fr

(*Received 15 June 1997; accepted 29 September 1997*)

An imaging experiment using a two-plane focusing refractive lens made of aluminium and operated in the hard X-ray range is described. The lens is made of a series of 1 and 0.8 mm-diameter lenses drilled through a 2 mm aluminium plate. It is exposed to the white beam from an undulator with total power as high as 1.7 kW and normal-incidence power density of 100 W mm^{-2}. The measured r.m.s. size of the image is 0.12 × 0.06 mm at a photon energy of 30 keV. Theoretical estimates for the transmission, aperture and tolerance of alignment of such lenses are made. It is found that the aperture of the lens is dominated by photoelectric absorption (Compton scattering) in the low (high) energy range of the spectrum. Beryllium is the most promising material.

Keywords: X-ray focusing; refractive lenses; imaging.

1. Introduction

The focusing of X-rays is usually made using bent crystals, curved mirrors, Fresnel and Bragg–Fresnel zone plates, and capillary optics (Hastings *et al.*, 1995; Kumakhov & Sharov, 1992). Several authors have been considering the use of refractive lenses in the X-ray range of the spectrum (Kirkpatrick & Baez, 1948; Suehiro *et al.*, 1991; Michette, 1991) and have been discouraged by the weak refractive part of the index combined with the rather large absorption. Recently, a simple type of refractive lens has been proposed and successfully tested in the X-ray range with a photon energy of 14 keV (Snigirev *et al.*, 1996). Such lenses are made by drilling a series of small holes with a diameter of the order of a millimetre in a low-Z material such as aluminium. These lenses are expected to be resistant to heat load and simple to build resulting in an astonishing low cost.

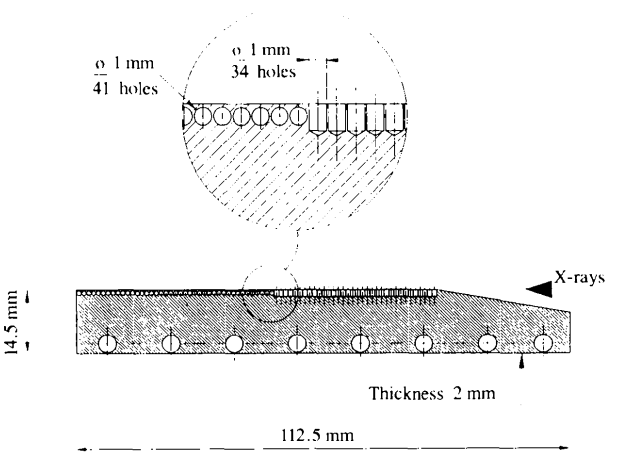

Figure 1
Drawing of the two-plane refractive lens used in ID6. The input face is set at a grazing angle to spread the heat load.

Their drawbacks are their limitation to high photon energies above 4 keV due to absorption, their strong chromatic aberrations and low aperture. However, they appear extremely well suited to the focusing of the undulator radiation of the new hard-X-ray third-generation synchrotron sources such as the ESRF, APS and SPring-8. The object of this paper is to report on the results of some tests and to discuss the potentialities of these lenses.

2. Description of the experiment

The original interest for these tests was the imaging of the electron beam sizes at the source of the undulator in the ID6 Machine Diagnostics beamline as a complementary emittance diagnostic. To do so, a lens was built by drilling 34 holes of 1 mm diameter with a vertical axis followed by 41 holes of the same diameter with an axis in the horizontal plane (see Fig. 1). The holes are drilled in a 2 mm-thick aluminium plate and are separated by 0.1 mm. As we shall see later, aluminium is not the best material but it was selected for its reasonably low Z value, easy machining and short-term delivery. The vertical source size in the middle of the undulator is ~10 μm r.m.s. for the 40 pm rad emittance routinely achieved. For a proper magnification of the source, one needs to place the lens as close as possible to the source, which conflicts with the severe heat load. In all cases water cooling is essential. The only places where sufficient water cooling is available on the ID6 beamline are the X-ray beam-position monitor motorized stages located at a distance of 22 m from the source. The design of the lenses was strongly inspired from the design of the tungsten blade of the X-ray beam-position monitor (Loyer, 1993) for which severe heat-load problems have been carefully studied and solved. The shape of the lens is shown in Fig. 1. The eight

lower large-diameter holes are used for clamping. Of the 14.5 mm height of the lens, only the upper 5 mm emerge from the heavily cooled copper fastener. The entrance face of the lens is inclined at some low incidence angle to spread the heat load and reduce the local temperature of the lens at the point of impact of the X-rays. After passing through the lens the X-rays travel through the graphite/beryllium window assembly placed in the front-end part of the beamline. The transmitted beam is then monochromated by a 311 silicon crystal diffracting in the horizontal plane (see Fig. 2). The monochromatic beam is converted to visible light by means of a 1 mm-thick CsI(Ti) scintillator and imaged by a CCD video camera. The whole experiment was controlled and performed from the storage ring control room. The scintillator is placed at 32.2 m from the middle of the ID6 straight section. Such an imaging set-up has been in use for more than 4 years in the ID6 beamline and for more than 2 years as the primary emittance diagnostic of the electron beam (Tarazona & Elleaume, 1995). The image of the X-ray beam when the monochromator is precisely tuned to the photon energy of one of the harmonics of the undulator spectrum on the axis of the electron beam is essentially an intense ellipsoidal spot. This spot is the footprint of the undulator central cone on the scintillator. The focusing of the lens in both the horizontal and vertical planes was selected for minimizing the spot size of the image at a photon energy of 25 keV. A different number of holes were used for focusing in the horizontal plane. This is due to the large β-function of the source (low divergence of the photon beam) responsible for a small violation of the geometrical optics laws (the same as for visible lasers). The undulator used for this experiment is a single segment of 36 periods of 46 mm. The spectrum is tunable with a deflection parameter K between 0 and 2.2. The experiment has been performed at a full ring current of 200 mA with a gap ranging from 20 to 40 mm corresponding to a maximum angle-integrated power of 1.7 kW and a normal-incidence power density as high as 100 W mm^{-2} at the position of the lens.

Table 1
Measured r.m.s. photon beam size with and without the lens.

	R.m.s. horizontal spot size (mm)	R.m.s. vertical spot size (mm)
No lens	0.60	0.30
29.5 keV	0.12	0.058
27.5 keV	0.11	0.056
25 keV	0.11	0.061

3. Results

Fig. 3 presents the image of the seventh harmonic of the undulator at a photon energy of 29.5 keV before insertion of the lens. The r.m.s. horizontal and vertical sizes were measured to be 0.55 and 0.30 mm, respectively, in good agreement with the β-function and emittance deduced from the pinhole camera (Elleaume *et al.*, 1995). The horizontal lines are produced by the unpolished beryllium window and graphite filters located 2 m downstream from the lens. Fig. 4 presents the same image after insertion of the lens and removal of some attenuation. The central spot originates from the focusing of the lens in both the horizontal and vertical planes. As expected, the spot can be displaced on the camera by moving the lens and vanishes for large displacements of the lens due to stronger absorption in the aluminium. Table 1 summarizes the measured r.m.s. sizes.

These results are quite encouraging. Horizontally the expected spot size is 0.11 mm. However, one would have expected a 0.010 mm r.m.s. vertical spot size around 25 keV. This discrepancy is not yet understood and several explanations are being studied. The most likely explanations are the non-perfectly cylindrical shape (as observed through a visible-light microscope) of the holes and/or inhomogeneities of the material.

4. Optimization

The results presented above are preliminary and further investigations and development are required to understand

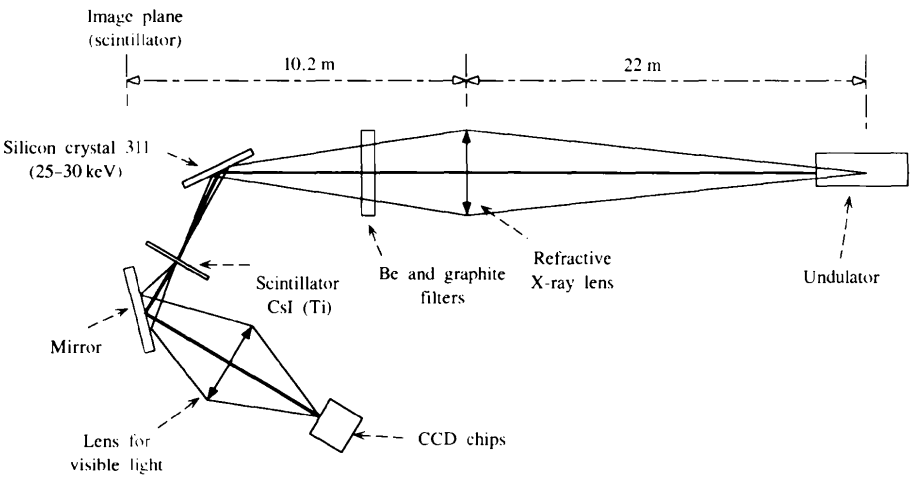

Figure 2
Schematic layout of the beamline set-up used to image the X-ray beam at the centre of the undulator.

all aspects fully. It is nevertheless important to stress the large potentialities of such lenses in many areas. Before enumerating them, let us briefly summarize the few equations that would allow anyone to optimize such a lens. I shall use the following definition of the real and imaginary parts of the index of a material,

$$n = 1 - \delta + i\beta. \tag{1}$$

β characterizes the absorption. It is related to the wavelength of the radiation, λ, and the absorption length, l_a, by the relation

$$\beta = \lambda/4\pi l_a = \lambda\rho/4\pi\mu, \tag{2}$$

where μ is the mass absorption coefficient in g cm^{-2}, which also depends on the photon energy, and ρ is the density of the material in g cm^{-3}. δ characterizes the refractivity. It can be expressed as (Vaughan, 1985)

$$\delta = f_1 r_0 \lambda^2 N_A \rho/2\pi A \simeq Z r_0 \lambda^2 N_A \rho/2\pi A, \tag{3}$$

where r_0 is the classical radius of the electron and N_A is the Avogadro constant. Z, A and ρ depend on the material; they are the number of electrons, the atomic weight and the density, respectively. f_1 is the real part of the atomic scattering factor, which for the low-Z material exposed to hard X-rays is approximated by Z. The focal length, F, produced by an array of N holes of radius R, is known from the geometrical optics as

$$1/F = 2N\delta/R. \tag{4}$$

Note the proportionality of δ, and therefore of $1/F$, on the square of the wavelength. These lenses suffer from strong chromatic aberration (in the sense of visible optics). If used for a microfocusing experiment, such lenses can only operate in conjunction with a monochromator (crystal or multilayer). It is important to study the transmission of the radiation through such a lens. Let us assume that the minimum distance between two adjacent holes is d and consider a beam propagating parallel to the line joining the centre of the hole of a single-plane focusing lens but displaced by a value x. The transmission of the radiation through such a lens for x smaller than the radius R can be approximated by

$$T(x) \simeq \exp[-Nd(4\pi\beta/\lambda + 1/l_s) - x^2/2\Sigma^2], \tag{5}$$

where Σ is the aperture of the lens given by

$$\Sigma^2 = \delta\lambda F/[4\pi\beta + (\lambda/l_s)] = \delta l_t F. \tag{6}$$

Here l_s is the attenuation length due to scattering and l_t is the total attenuation length due to absorption and scattering. At a sufficiently low energy, the attenuation by absorption, $4\pi\beta/\lambda$, dominates the attenuation by scattering, l_s, while at high energies l_s dominates with a most important contribution from Compton scattering. The on-axis transmission, $T(0,0)$, and total transmission, T, of a Gaussian photon beam with horizontal and vertical r.m.s. sizes σ_x and σ_z through a two-plane focusing lens with apertures Σ_x and Σ_z are

$$T(0,0) = \exp[(-Nd + D)/l_t],$$

$$T = \int_{-\infty}^{\infty}\int_{-\infty}^{\infty} T(x,z)\,dx\,dz = T(0,0)/\{[1 + (\sigma_x/\Sigma_x)^2]^{1/2}[1 + (\sigma_z/\Sigma_z)^2]^{1/2}\}, \tag{7}$$

where N is the total number of holes (vertical and horizontal) and D is an extra thickness of material introduced at the extremities due to the grazing-incidence input face (see Fig. 1). The r.m.s. beam size of the transmitted beam, σ_t, is deduced from the r.m.s. input size, σ, and the aperture, Σ, by

$$\sigma_t = \sigma/[1 + (\sigma/\Sigma)^2]^{1/2}. \tag{8}$$

It is clear from (7) that to maximize the transmission one should drill a small number of holes as close as possible to each other and design the lens with a sufficiently large aperture, Σ. Equation (6) shows that the square of the aperture of such lenses is the product of a geometrical term, λF, multiplied by a term which depends on the material and the wavelength. Fig. 5 presents the r.m.s. aperture for beryllium, carbon and aluminium computed from (6) as a function of the photon energy for a focal length of 10 m. Clearly, the low-Z material shows a larger aperture at low energy while at very high energies, due to the dominance of

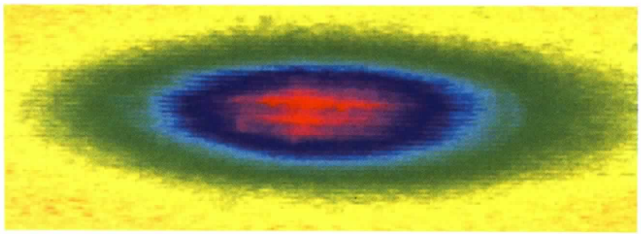

Figure 3
Spot size of the seventh harmonic of the undulator at 29.5 keV observed at a distance of 32.2 m without the lens. The r.m.s. sizes are 0.55 and 0.30 mm, in good agreement with the emittance derived from the pinhole camera and the β-function of the source point.

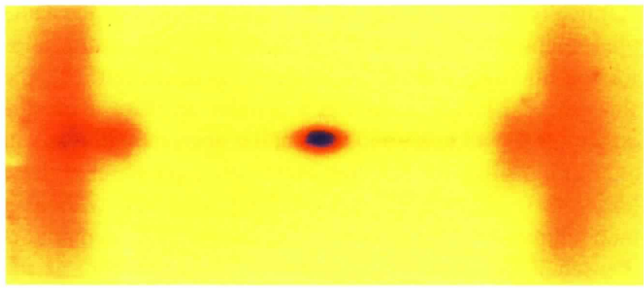

Figure 4
Same image conditions as in Fig. 2 after insertion of the lens and removal of some attenuation. The central spot is the result of focusing of the radiation by the refractive lens. Some radiation is visible on the right- and left-hand side which is not passing through the lens.

Compton scattering, the apertures are similar. For precise imaging, spherical aberrations are an important issue. While a complete treatment of the spherical aberrations (analytical or by ray tracing) is out of the scope of this presentation, one can nevertheless summarize the principle results. Spherical aberrations are important for the rays propagating at a distance x close to the radius, R. The extent to which spherical aberrations should be avoided depends on the required spot size in the image plane. The figure of merit is the ratio of the r.m.s. transmitted beam, σ_t, over the radius, R, which should be small. Finally, it is important to stress that these lenses operate at almost normal incidence; they are therefore much more tolerant than mirrors to any slope error that may be due to machining and heat load. One easily understands this by expressing the refraction condition at the interface between the air and the material. Let α be the surface angle error, then the angle error, θ, induced by the refracted beam impinging on a surface with angle i with respect to the normal is

$$\theta \simeq \delta\alpha / \cos^2(i). \tag{9}$$

Clearly, θ is minimum at normal incidence and diverges at grazing incidence. In this respect the shaping introduced at the entrance of the lens to spread the heat load should be kept to the minimum required to limit the aberration produced. δ is of the order of a few 10^{-7}, therefore a large angle error, α, on a normal-incidence interface will have very limited consequences on the transmission angle, θ. In particular, surface deformation under heat load only affects the entrance interface and should have little effect on the size of the image. Focusing of the ray occurs by the cumulation of many small angles taking place in each hole, and having a single hole with a different shape than the others will not make a big difference to the total angle. As a matter of fact, in an experiment with such aluminium lenses improperly shaped to withstand the heat load from the undulator beam, we observed some melting of the input face resulting in an almost complete disappearance of the first five holes without any dramatic change in the focusing properties of the lens.

The tolerance of positioning of the X-ray beam with respect to the lens is a fraction of the r.m.s. transmitted beam, σ_t. The tolerance for the angular positioning of the lens with respect to the X-ray beam is a fraction of the inverse of the total number of holes, which is very easily achieved.

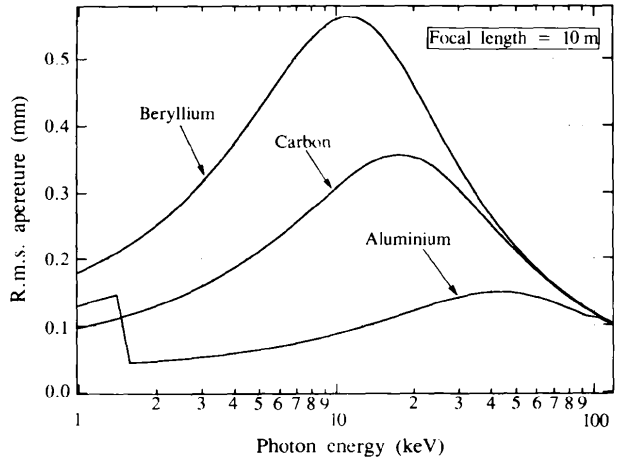

Figure 5
R.m.s. aperture of a refractive lens made of beryllium, carbon or aluminium as a function of the photon energy assuming a focal length of 10 m. The computation takes into account photoelectric absorption, and coherent and incoherent (Compton) scattering. The aperture at low (high) energy is essentially determined by photoelectric absorption (Compton) scattering.

5. Discussion

For 30 keV radiation the focal length of the lens is 12.2 m (10.2 m) in the horizontal (vertical) plane. As a result, the corresponding aperture, Σ, is 0.16 mm (0.14 mm), to be compared with the r.m.s. beam size, σ, of the central cone of 0.45 mm (0.12 mm). The minimum thickness of aluminium is $0.1 \times (34 + 41) + 4.2 = 11.7$ mm. Consequently, the overall transmission is 0.07 (material transmission) $\times$ 0.34 (horizontal aperture) $\times$ 0.76 (vertical aperture) = 0.018, which is in good agreement with our observations. This lens has not yet been fully optimized and a higher transmission could have been obtained by further reducing the spacing between each hole. If one replaces the aluminium with beryllium with the same hole radius and shape but a larger number of holes to achieve the same focal length, the overall transmission is 0.31, 0.31 and 0.16 at photon energies of 30, 15 and 10 keV, respectively. In addition, the temperature rise of the beryllium would be reduced due to its lower absorption. Other low-Z materials are worth studying, such as graphite, boron nitride or boron carbide. To improve the transmission of such lenses, one must reduce the minimum thickness of material ($Nd + D$) and/or reduce the r.m.s. beam size of the photon beam, σ, which requires the placement of such lenses closer to the undulator. Note that the optimization of such lenses for a simple 1:1 imaging ratio is quite different from that of a microfocus of, for example, a 30:1 ratio. A microfocus lens is typically placed at twice the distance from the source compared with the 1:1 lens. The radius of the hole is therefore twice as large to scale identically to the spot size of the central cone. For the same photon energy there will therefore be 60 times more holes for the microfocus lens. In addition, from (5) and (6), the shorter focal length results in a smaller aperture. Both the larger number of holes and the smaller aperture will result in a lower transmission. Another important application of these lenses is in the use of the undulator spectrum without a monochromator. The photon energy from each harmonic is focused differently. If one places a small aperture at the imaging plane of a specific harmonic, one would discriminate the other harmonics. The transmitted spectrum would be that of the selected harmonics with all the others attenuated. The lower the number of the selected harmonic, the more efficient is the harmonic discrimination. The resulting photon flux per unit area over a 1% bandwidth is

several orders of magnitude higher than that presently achieved. Each lens is optimized for a specific photon energy, but operation over a large energy range can be achieved by installing an array of such lenses on a movable stage. A user would select a lens according to the application. The X-ray beam-position monitor set-up presently in place in the ID6 beamline and optimized for a different goal (beam-position measurement) allows the insertion of four different lenses without any modification. The power per unit area on the sample or monochromator located at the image plane should not be significantly modified by the presence of the lens since only a small fraction of the spectrum is focused to a narrow size and part of the power is deposited in the lens itself. Obviously to approach these performances a number of issues need to be properly addressed, such as the constraints induced by heat load, stability of the lens-positioning system, required homogeneity and low roughness of the material *etc.*

6. Conclusions

This paper presents a theoretical investigation of the transmission and aperture of refractive lenses. However, a full treatment of spherical aberrations by ray tracing or analytical methods allowing a determination of the tolerance for the hole alignment is still needed. At the current state of the art these lenses have experimentally turned out to be practical for the monitoring of high-power undulator beams. Even though their focal length depends on the photon energy and their transmission suffers from absorption and scattering of the material, they offer a very inexpensive and highly flexible alternative to conventional focusing mirrors. Single- or two-plane focusing X-ray lenses made of beryllium provide an easy way to optimize the ESRF undulator beamlines further.

Note that in the course of writing and correcting the paper, I have been informed of other results: A. Snigirev achieved a 18 × 8 μm spot size on a two-plane focusing lens at 30 keV with a focal length of 2 m made with 200 holes. Experiments with single-plane focusing beryllium lenses made on ID16 by M. Krisch and F. Sette show an increase of 5.9 of the flux in the image plane integrated inside a 50 μm aperture for a photon energy of 13.8 keV. Experiments on the ID6 beamline of the ESRF with a two-plane focusing beryllium lens at 25 keV show an increase of the flux per unit area by a factor of 20 at 32 m from the source after inserting a beryllium lens.

The author wishes to thank A. Snigirev for stimulating discussions, D. Gamonet and the front-end group who installed the lens in the vacuum.

References

Elleaume, P., Fortgang, C., Penel, C. & Tarazona, E. (1995). *J. Synchrotron Rad.* **2**, 209–214.
Hastings, J. B., Hubbert, S. L. & Williams, G. P. (1995). *Rev. Sci. Instrum.* **66**, 1271–2390.
Kirkpatrick, P. & Baez, A. (1948). *J. Opt. Soc. Am.* **38**, 766.
Kumakhov, M. A. & Sharov, V. A. (1992). *Nature (London)*, **357**, 390–391.
Loyer, F. (1993). *DIPAC'93 Conf.*, Montreux, Switzerland, May 1993.
Michette, A. G. (1991). *Nature (London)*, **353**, 510.
Snigirev, A., Kohn, V., Snigireva, I. & Lengeler, B. (1996). *Nature (London)*, **384**, 49–51.
Suehiro, S., Miyaji, H. & Hayashi, H. (1991). *Nature (London)*, **352**, 385–386.
Tarazona, E. & Elleaume, P. (1995). *Rev. Sci. Instrum.* **66**, 1974–1977.
Vaughan, D. (1985). Editor. *X-ray Data Booklet*, LBL PUB-490, §2–7. Lawrence Berkeley Laboratory, USA.